CUSTOMER STORY // AEROSPACE INDUSTRY

FATIGUE VERIFICATION OF HIGH LOADED BOLTS OF A ROCKET COMBUSTION CHAMBER

Sensitivity analyses and robustness evaluations with optiSLang including dynamic load conditions during flight operation help to verify high quality standards of bolt connections.

Introduction

Rocket engines and the bolted interfaces between their components have to withstand intense thermal and structural loads. Therefore, particular emphasis is placed on the quality assurance and verification from incoming inspection of the fasteners. During these tests, a fatigue analysis is performed to ensure a high bolt durability covering the dynamic loads during the engine's operation. However, there is a significant difference between test and flight loads leading to a non-linear relation between test results and expected operational life. A sensitivity analysis is conducted to generate a linking, multi-parametrical model that can be adapted to both load cases. While the parameters scatter within the unifying parameter set, the life expectation also varies for both load cases. Accordingly, a robustness analysis is finally performed to project the result variety under flight conditions onto the test result scattering.

Bolts or screws connect constructional parts with each other. The threaded bolt shaft and its evenly shaped counterpart nut or threaded blind hole transmit forces by a shapeclosed connection. In the case of overloading, the bolt will fail and lose its force transmitting capability.

A bolt can be overloaded by stressing leading to ductile failure, preferably at the first thread in contact. Another overloading mechanism is known as critical fatigue after the exposure to a certain number of load cycles. The second will be outlined in this article.

Basics on bolt analysis

Pretension

During bolt mounting into a blind hole or a nut, pretension has to be generated. Continuous torque tightening increases bolt and flange force at the same rate, while the value of deformation depends on the stiffness of both components. Due to the tension load, the bolt is strained by the law of elasticity $\Delta l_B = F_B/K_B$ with the bolt force F_B and the bolt's rigidity K_B that leads to the absolute bolt deformation Δl_B. With the same force F_B but a different flange stiffness K_F, the flange parts are compressed about $\Delta l_F = F_B/K_F$. Here Δl_F denotes the deformation of the flange area in an imaginary cylinder between the bolt head and the nut. K_F is the corresponding flange stiffness.

The mounted and pre-stressed interface is loaded by the operational force F_L. If F_L is oriented in tension direction, the bolt will be additionally stressed while the flange compression decreases. Hence the operational load is taken by both components depending on their stiffness. The ratio between the force fraction taken by flange decompression F_{LF} and the part covered by the bolt F_{LB} is defined by the force ratio Φ:

$$\Phi = \frac{K_B}{K_B + K_F} = \frac{F_{LB}}{F_L} \qquad (1)$$

The bolt and flange behavior due to pretension and operational load is illustrated in Figure 1.

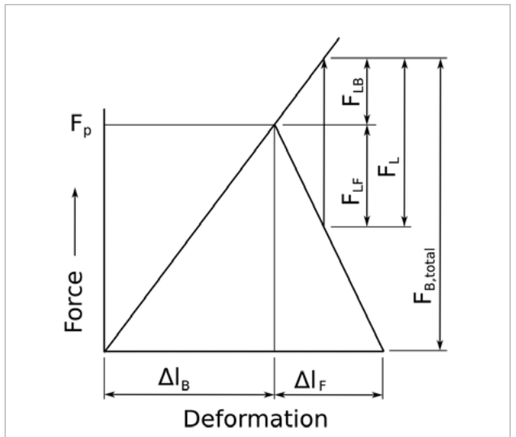

Fig. 1: Load-deformation-curve of a classical bolt connection

The effect of the force ratio becomes substantial for dynamic loading domains. The high durability of bolted joints is to be attributed to Φ and the fact that an operational load is partly taken by the relief of the pre-stressed flanges. The higher the flange stiffness compared to the stiffness of the bolt shaft, the lower the actual impact on operational loads stressing the bolt. This effect is related to equation (1). This advantageous behavior decreases the bolt stress range per cycle which crucially increases the bolt life.

Stress distribution

Loaded by an axial force F_{ax}, the nominal stress σ_{nom} within the bolt shaft equals to:

$$\sigma_{nom} = \frac{F_{ax}}{A_{st}} \qquad (2)$$

with A_{st} as stress area.

Notch effects at the thread ground lead to a local stress concentration $\sigma_{max} = K \cdot \sigma_{nom}$. The stress concentration factor K depends, among other things, on the depth of the thread and the radius of the thread ground. To estimate the magnitude of K, tables are presented in engineering literature, e.g. Young and Budynas [2002]. As a result of the stress concentration at the thread grounds, a stress distribution equivalent to Figure 2 occurs.

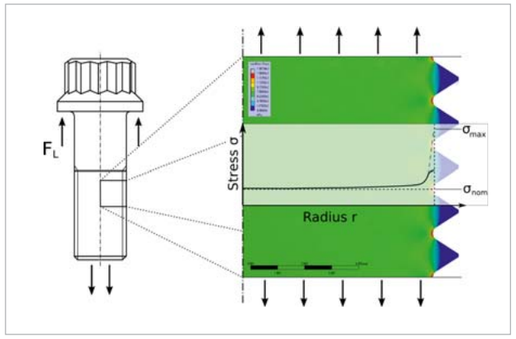

Fig. 2: Stress distribution along threaded bolt and stress concentration at thread grounds

When the locally increased stress reaches the yield limit σ_y, local plastic deformations occur. For this study, the Neuber rule is used to approximate the magnitude of plastic deformation. Neuber expects a hyperbola in the stress-strain field where the generation of stress and strain stays constant $\sigma\varepsilon = \sigma_{max}^2/E$. When the Neuber hyperbola fits the endpoint of the linear extrapolated stress-strain line $\sigma_{max,el}$, it crosses the yield curve at the point $\sigma_{max,Neuber}$. This point approximates the stress-strain relation after yielding as shown in Figure 3. As a yield curve, a bilinear approximation is used. It is defined by the yield limit $(R_{p0.2}/E, R_{p0.2})$ at ultimate conditions (A, R_M).

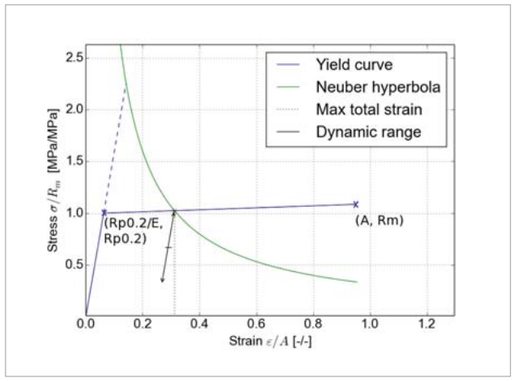

Fig. 3: Plastic stress-strain state obtained by Neuber approximation

Fatigue damage

The bolt life prediction is realized by the Coffin Manson approach. With the universal slope proposed by Lemaitre and Chaboche [1990]:

$$\Delta\varepsilon_{\text{univ.}} = f(N_f) = 3.5\frac{R_m - \sigma_m}{E} \cdot N_f^{-0.12} + D_u^{0.6} \cdot N_f^{-0.6} \qquad (3)$$

the total strain range $\Delta\varepsilon$ is related to the number of cycles until failure N_f. R_m being the ultimate strength, D_u is the ductility of the material and σ_m is the mean stress of the load cycle.

Herein, the values in the exponents are fitted to a wide range of different materials for universal validity. To reach our needs, these constants are considered as material specific and are chosen in accordance to the bolt material. A better adjustable form of (3) is used with the parameters C_1 to C_4 that can be fitted to the actual material behavior:

$$\Delta\varepsilon = f(N_f) = C_1\frac{R_m - \sigma_m}{E} \cdot N_f^{-C_2} + D_u^{C_3} \cdot N_f^{-C_4} \qquad (4)$$

Aligned values for C_1 to C_4 can be found for different materials in Lemaitre and Chaboche [1990]. Varying the constants C_1 to C_4 of (4), it influences the $\Delta\varepsilon - N_f-$ Curve as shown in Figure 4. The actual sensitivity of the model towards these Coffin Manson parameters is analyzed in section 4.

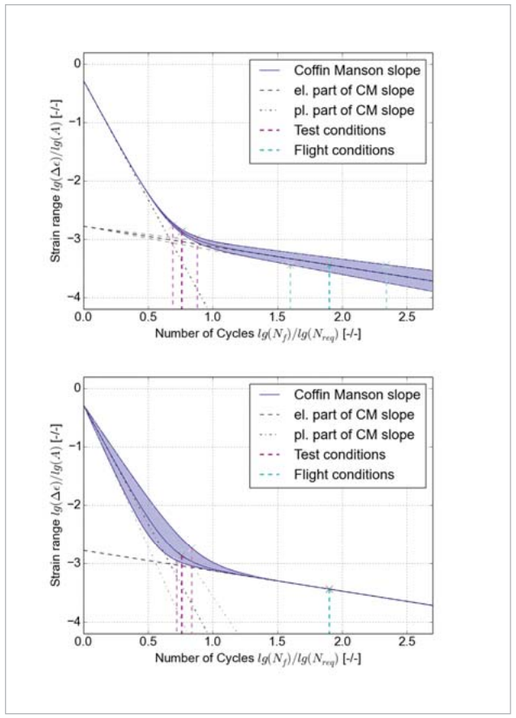

Fig. 4: Coffin Mansons fatigue curve - variety of the constants C_2 and C_4 are shown by the diffuse bluish areas

Bolt validation procedure and uncertainties

To accept the bolts for flight application, a few per batch are submitted to several different test procedures. The check regarding fatigue failure is performed by a cycling test. It is known that the load conditions during the test differ to those experienced during the rocket launch. The objective of this investigation was to correlate the results of the fatigue test with the circumstances of real operation. Finally, it had to be shown that the required cycles during the flight can be validated by a certain number of test cycles.

Validation test conditions

For fatigue testing, the bolt was inserted into the testing device with contact at the thread and bolt head. No flange material was considered. Loads applied by the device were fully covered by the bolt itself. The full range of alternating testing loads were applied to the bolt. The diagram in Figure 5a (see next page) displays the load-deformation curve of this behavior.

The large load range of $2F_a$ combined with the stress concentration factor at the thread ground lead to a local cyclic plastification as shown in Figure 2. According to the Neuber approximation, this opened the stress-strain hysteresis, stretched the stress range and reduced the bolt life significantly.

Flight conditions

The considered bolts connect the combustion chamber to the injector. During mounting, a high pretension F_p was applied to avoid interface sliding. The dynamic interface loads F_L occurred in a moderate level which lead to a relatively low alternating bolt force F_a compared to the pretension force F_p. The ratio can be seen in the load deformation curve in Figure 5b (see next page). With high flange stiffness, which was given in this case, the dynamic loads added to the pretension were mostly covered by flange relief. The actual bolt load F_a alternated in a much smaller stress range compared to the test case. That lead to a solely elastic dynamic behavior with a lesser strain range. According to Coffin Manson and shown in Figure 4, a small $\Delta\varepsilon$- resulted in a significantly longer bolt life than under test conditions.

Correlation of test results to flight conditions

To compare test results with flight live expectations, the mentioned influences needed to be considered. Slight uncertainties of yield stress $R_{p0,2}$ and strain at rupture A lead to contrary changes in the calculation of the strain range via the Neuber approximation approach. This exceeded the resulting live expectation. Additional uncertainties occurred by varying the Coffin Manson coefficients C_1 to C_4. Also, the stress concentration factor of the threat K was not a definite value but depended on geometrical width ratio and the edge radius which was not definitely detectable. It was treated as a variable during the following investigations.

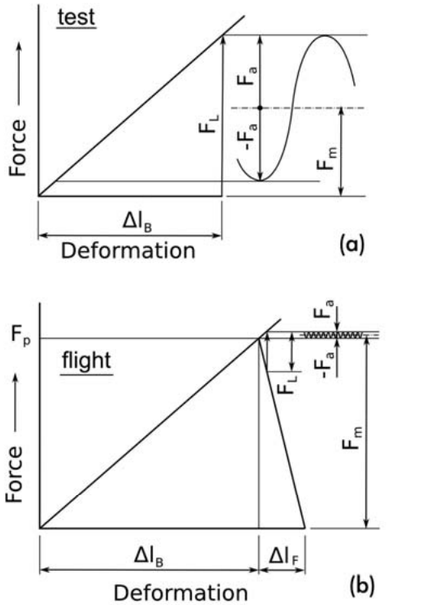

Fig. 5: Load-deformation-curve under a) test conditions and b) flight conditions

Life expectations were calculated by considering a certain set of the mentioned variables. Each parameter set had two results:

- $N_{f,test}$ – life expectation under test conditions and
- $N_{f,flight}$ – life expectation during the flight

Finally, it had to be shown that the flight requirement was reached in all cases, which meant in any possible combination of input variables. Parameter combinations that lead to lower life expectation needed to be excluded by the choice of the test conditions.

Robustness under flight conditions

All possible variables influencing the bolt's life expectation were analyzed. After performing a sensitivity analysis with optiSLang, it could be seen that the influence of parameters varied from flight to test case. The test case showed the highest sensitivity to the Coffin Manson variables C_1 and C_2 that were responsible for the high cycle domain of the slope.

For the flight case, these variables had a minor impact. Despite to its small strain range $\Delta\varepsilon_{\text{flight}}$, the sensitivity was mostly strength driven. $R_{p0.2}$ and R_m were the most influencing parameters in this case. Table 1 lists the sensitivities for both cases.

Parameter	unit	Test	Flight
A_m	[%]	0	1
E	$[^{MPa}/_{MPa}]$	0	0
K	[%]	1	4
$R_{p0.2}$	$[^{MPa}/_{MPa}]$	9	36
R_m	$[^{MPa}/_{MPa}]$	16	58
C_1	[%]	47	3
C_2	[%]	17	5
C_3	[%]	1	0
C_4	[%]	6	0

Table 1: Model sensitivity under test and flight conditions towards input parameters

Considering the influencing parameters as normally distributed, the model was fed with specific parameter sets. The distribution of the parameters was evaluated from test data, or, in the case of the Coffin Manson variables, from literature. For each input set, an output of the two life expectations was obtained – one for test and one for flight.

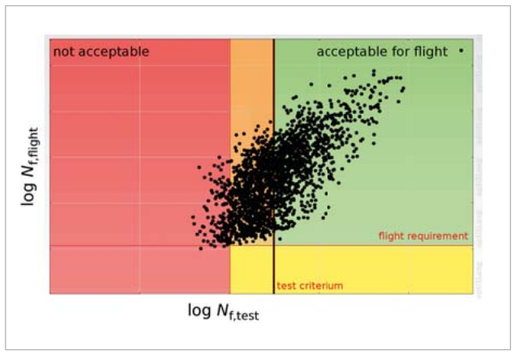

Fig. 6: Criteria for fatigue test

With optiSLang, a robustness analysis was executed. As a result of the life evaluation, the plot shown in Figure 6 was drawn. It shows the life results of 5000 parameter sets. For each set, the expected flight life was prognosticated for a calculated test life. As a requirement for flight acceptance, the bolts had to withstand the specified loads, even with the worst possible combination of material parameters. As shown in Figure 6, all points below the flight requirements were not accepted meaning all test results in the red area would lead to bolt rejection from flight worthiness. If one of the few tested bolts per incoming batch showed an unacceptable fatigue durability, the whole batch was not allowed to be mounted.

The actual test requirement was finally defined at a higher number of cycles during the test to meet an additional safety factor. Test results in the orange area (see Figure 6) could achieve acceptance level by performing additional analysis. The big plus of the indifferent orange area was the early recognition of any disadvantageous changes of production methods. If processes changed, the final product could be affected in a negative way. With the demanding test requirement, changes could be detected early and counteractions could be prepared.

The bolts that met the test requirement, illustrated by the green area in Figure 6, were accepted for flight without further analysis.

The acceptance regarding bolt life could finally be verified. With the possibility of taking all parameters into account within a single analysis, the understanding of its sensitivities was improved. Having the bandwidth of each parameter in mind, the spread of the bolt life expectation could be shown. In the anthill plot shown in Figure 6, this life expectation was projected on the durability under testing conditions. With the relations between flight and test, a new test criteria was found that disqualified unacceptable bolts before they went to flight.

Author // Marcus Lehmann, Dieter Hummel
(Airbus Defence & Space)

Literature // Jean Lemaitre and Jean-Louis Chaboche. Mechanics of solid materials. Cambridge university press, 1990./ Warren Clarence Young and Richard Gordon Budynas. Roark's formulas for stress and strain, volume 7. McGraw-Hill New York, 2002.